Direct Torque Control of Brushless DC Drives With Reduced Torque Ripple

Yong Liu, *Student Member, IEEE*, Z. Q. Zhu, *Senior Member, IEEE*, and David Howe

***Abstract*—The application of direct torque control (DTC) to brushless ac drives has been investigated extensively. This paper describes its application to brushless dc drives, and highlights the essential differences in its implementation, as regards torque estimation and the representation of the inverter voltage space vectors. Simulated and experimental results are presented, and it is shown that, compared with conventional current control, DTC results in reduced torque ripple and a faster dynamic response.**

***Index Terms*—Brushless dc (BLDC) drives, direct torque control (DTC), permanent-magnet motor.**

I. Introduction

THE permanent magnet brushless ac (BLAC) and brushless dc (BLDC) drives [1], [2] are used extensively for many applications, ranging from servos to traction drives. They differ primarily in their current and back-electromotive-force (EMF) waveforms. In a BLAC drive, the phase current is controlled by a pulsewidth-modulation (PWM) inverter to have a sinusoidal waveform and vector control is often employed, while in a BLDC drive, the PWM phase current has an essentially rectangular waveform. In theory, a permanent magnet brushless motor with any back-EMF waveform can be operated in either BLAC or BLDC mode, although, in practice, it is desirable for a BLAC motor to have a sinusoidal back-EMF waveform and BLDC motor to have a trapezoidal back-EMF waveform in order to minimize the torque ripple and maximize the efficiency and torque capability. A sinusoidal back-EMF waveform can be obtained by skewing the stator slots and/or rotor magnets, employing a distributed stator winding, shaping the magnets, or employing a sinusoidal magnetization distribution. BLDC motors often employ concentrated windings [2], since these result in shorter end windings, which is conducive to a high efficiency and torque density. Further, while BLAC drives require a precision rotor position sensor, such as encoder, BLDC drives only require discrete position sensors, such as Hall devices [1], [2]. Therefore, in general, BLDC drives are relatively low cost. This paper focuses on the control of such BLDC drives.

Paper IPCSD-05-005, presented at the 2004 Industry Applications Society Annual Meeting, Seattle, WA, October 3–7, and approved for publication in the IEEE TRANSACTIONS ON INDUSTRY APPLICATIONS by the Industrial Drives Committee of the IEEE Industry Applications Society. Manuscript submitted for review July 11, 2004 and released for publication January 26, 2005.

The authors are with the Department of Electronic and Electrical Engineering, University of Sheffield, Sheffield, S1 3JD, U.K. (e-mail: elp01YL@sheffield.ac.uk; Z.Q.ZHU@sheffield.ac.uk; D.Howe@sheffield.ac.uk).

Digital Object Identifier 10.1109/TIA.2005.844853

Generally, BLDC drives employ current control, which essentially assumes that the torque is proportional to the phase current. Since, in practice, the relationship is nonlinear, various current control strategies have been adopted to minimize torque pulsations, by employing pre-optimized waveforms for the reference current, for example. Such an optimal current excitation scheme was proposed in [3], which resulted in minimal copper loss and ripple-free torque from a BLDC drive. However, it was based on the d–q axes transformation, and could not respond to rapid torque changes. A current controller which estimated the electromagnetic torque from the rate of change of coenergy was described in [4]. However, in its implementation to a BLDC drive, the estimated torque was obtained from a lookup table, and the control algorithm did not directly involve flux control. An instantaneous torque controller based on variable structure control in the d–q reference frame was proposed in [5]–[7]. However, although experimental results showed that it was effective in reducing torque ripple, it was only applicable to three-phase BLDC operating in the 180° conduction mode, and not to the more usual 120° conduction mode. In [8], electromagnetic torque pulsations were reduced with a torque controller in which the torque was estimated from the product of the instantaneous back-EMF and current. However, the winding resistance was neglected and the inverter output voltage had to be calculated, which assumed that the back-EMF waveform was known. The real-time estimation of the back EMF, using the model reference adaptive method, was reported in [9], which also employed a variable-structure torque controller with space-vector PWM. However, it was only applied to a three-phase BLAC drive, and resulted in a relatively complex relationship between the output voltage in the q axis and the torque error.

Direct torque control (DTC) was originally developed for induction machine drives [10], [11], and directly controls the flux linkage and electromagnetic torque, considering the electrical machine, the power electronic inverter, and the control strategy at the system level. A relationship is established between the torque, the flux and the optimal inverter switching so as to achieve a fast torque response. It exhibits better dynamic performance than conventional control methods, such as vector control, is less sensitive to parameter variations, and is simpler to implement. DTC has been successfully applied to induction machines [10], [11], and, more recently, to BLAC machines [12], [13].

This paper considers the application of direct torque control, to a three-phase BLDC drive operating in the 120° conduction mode (i.e. two phases conducting) to achieve instantaneous

torque control and reduced torque ripple. As will be shown, the essential differences between the DTC of BLDC and BLAC drives are in the torque calculation and the representation of the voltage space vectors. Simulated and experimental results are presented to illustrate the application of DTC to a BLDC drive.

II. DTC of BLAC and BLDC Drives

In general, neglecting the influence of mutual coupling between the direct and quadrature axes, the electromagnetic torque of a permanent-magnet brushless machine in the synchronously rotating d–q reference frame can be expressed as [9], [14], [15]

$$T_e = \frac{3}{2}\frac{p}{2}\left[\left(\frac{dL_d}{d\theta_e}i_{sd} + \frac{d\psi_{rd}}{d\theta_e} - \psi_{sq}\right)i_{sd} + \left(\frac{dL_q}{d\theta_e}i_{sq} + \frac{d\psi_{rq}}{d\theta_e} + \psi_{sd}\right)i_{sq}\right] \quad (1)$$

where

$$\psi_{sd} = L_d i_{sd} + \psi_{rd} \quad (2)$$

$$\psi_{sq} = L_q i_{sq} + \psi_{rq} \quad (3)$$

and θ_e is the rotor electrical angle, p is the number of poles, i_{sd} and i_{sq} are the d- and q-axes currents, L_d and L_q are the d- and q-axes inductances, respectively, and ψ_{rd}, ψ_{rq}, ψ_{sd}, and ψ_{sq} are the d- and q-axes rotor and stator flux linkages, respectively.

After a d–q transformation, a fundamental component of flux linkage is transformed into a dc component, while 5th and 7th harmonics transform into 6th harmonics, 11th and 13th harmonics transform into 12th harmonics, 17th and 19th harmonics transform into 18th harmonics, and so on. Thus, for a machine having a sinusoidal permanent-magnet flux, $\psi_{rd} = \text{constant}$ and $\psi_{rq} = 0$. However, for nonsinusoidal flux, ψ_{rd} is composed of a dc component and 6th, 12th, 18th harmonics, etc., while ψ_{rq} consists of 6th, 12th, 18th harmonics, etc.

Torque pulsations are associated mainly with the flux harmonics, the influence of higher order harmonics in the stator winding inductance usually being negligible [16]. Therefore, for machines equipped with a surface-mounted magnet rotor (i.e., nonsalient), it can be assumed that L_d and L_q are constant, i.e., $L_d = L_{d0}$, $L_q = L_{q0}$, and the electromagnetic torque can be expressed as

$$T_e = \frac{3}{2}\frac{p}{2}\left[\left(\frac{d\psi_{rd}}{d\theta_e} - \psi_{rq}\right)i_{sd} + \left(\frac{d\psi_{rq}}{d\theta_e} + \psi_{rd}\right)i_{sq} + (L_{d0} - L_{q0})i_{sq}i_{sd}\right]. \quad (4)$$

At this stage, it is worth considering the following cases.

1) When the stator flux linkage due to the permanent magnets varies sinusoidally, ψ_{rd} is constant, $\psi_{rq} = 0$, $d\psi_{rd}/d\theta_e = 0$, and $d\psi_{rq}/d\theta_e = 0$. The electromagnetic torque equation, for both BLAC and BLDC operation, with either a nonsalient- or salient-pole rotor, can then be simplified as

$$T_e = \frac{3}{2}\frac{p}{2}(\psi_{sd}i_{sq} - \psi_{sq}i_{sd}) \quad (5)$$

or, in the stationary α–β reference frame, as

$$T_e = \frac{3}{2}\frac{p}{2}(\psi_{s\alpha}i_{s\beta} - \psi_{s\beta}i_{s\alpha}) \quad (6)$$

where i_{sa}, $i_{s\beta}$, ψ_{sa}, and $\psi_{s\beta}$ are the α- and β-axes stator currents and flux linkages, respectively, viz.

$$\psi_{s\alpha} = \psi_{sd}\cos\theta_e - \psi_{sq}\sin\theta_e \quad (7)$$

$$\psi_{s\beta} = \psi_{sd}\sin\theta_e + \psi_{sq}\cos\theta_e \quad (8)$$

$$i_{s\alpha} = i_{sd}\cos\theta_e - i_{sq}\sin\theta_e \quad (9)$$

$$i_{s\beta} = i_{sd}\sin\theta_e + i_{sq}\cos\theta_e. \quad (10)$$

However, if the stator flux-linkage variation is nonsinusoidal, which is generally the case for BLDC machines, the general torque equation (1) must be employed, since $d\psi_{rd}/d\theta_e \neq 0$, $d\psi_{rq}/d\theta_e \neq 0$.

2) For nonsalient-pole brushless machines with a nonsinusoidal stator flux linkage, since $L_{d0} = L_{q0} = L_s$, the electromagnetic torque, for both BLAC and BLDC operation, can be simplified as

$$T_e = \frac{3}{2}\frac{p}{2}\left[\left(\frac{d\psi_{rd}}{d\theta_e} - \psi_{rq}\right)i_{sd} + \left(\frac{d\psi_{rq}}{d\theta_e} + \psi_{rd}\right)i_{sq}\right] \quad (11)$$

in the rotating d–q-axes reference frame, or as

$$T_e = \frac{3}{2}\frac{p}{2}\left[\frac{d\psi_{r\alpha}}{d\theta_e}i_{s\alpha} + \frac{d\psi_{r\beta}}{d\theta_e}i_{s\beta}\right] \quad (12)$$

in the stationary α–β reference frame, where ψ_{ra} and $\psi_{r\beta}$ are the α- and β-axes rotor flux linkages, respectively, viz.

$$\psi_{r\alpha} = \psi_{rd}\cos\theta_e - \psi_{rq}\sin\theta_e \quad (13)$$

$$\psi_{r\beta} = \psi_{rd}\sin\theta_e + \psi_{rq}\cos\theta_e. \quad (14)$$

However, for a nonsalient BLAC motor with a sinusoidal flux linkage, $\psi_{rd} = \psi_m$ and $\psi_{rq} = 0$, and the torque equation can be further simplified as

$$T_e = \frac{3}{2}\frac{p}{2}\psi_m i_{sq} \quad (15)$$

or, in the stationary reference frame as

$$T_e = \frac{3}{2}\frac{p}{2}(\psi_{s\alpha}i_{s\beta} - \psi_{s\beta}i_{s\alpha}) \quad (16)$$

which is the same as (6).

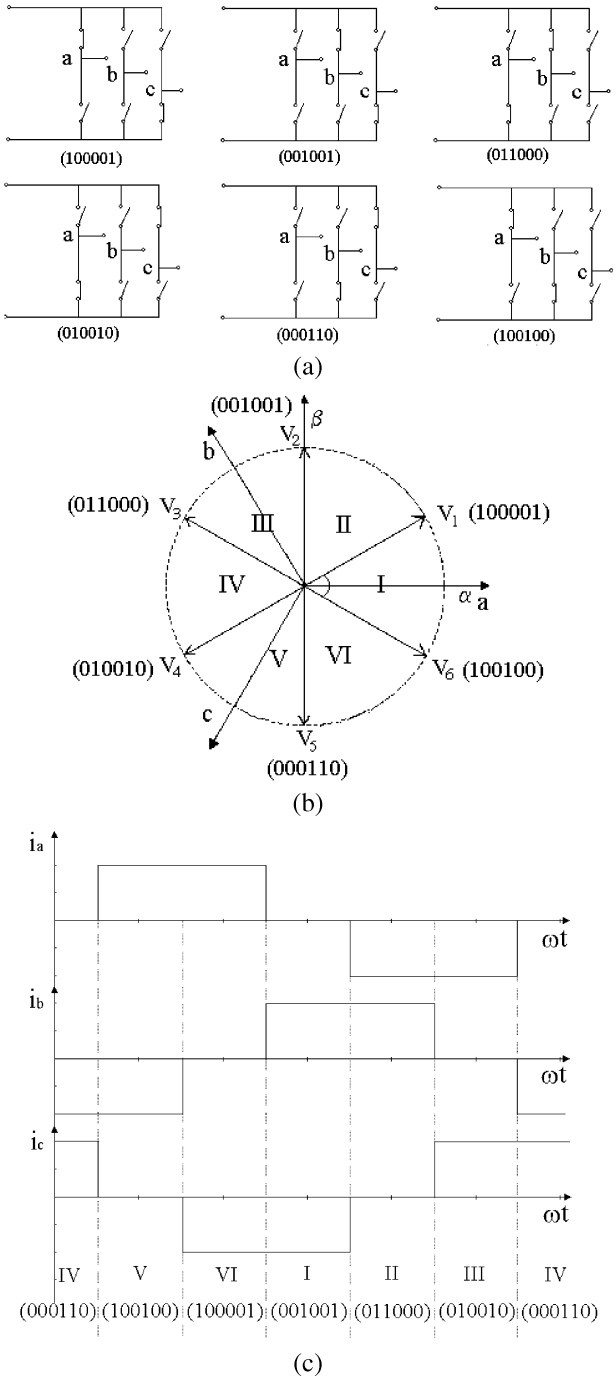

Fig. 1. Nonzero-voltage space vectors for BLDC drive.

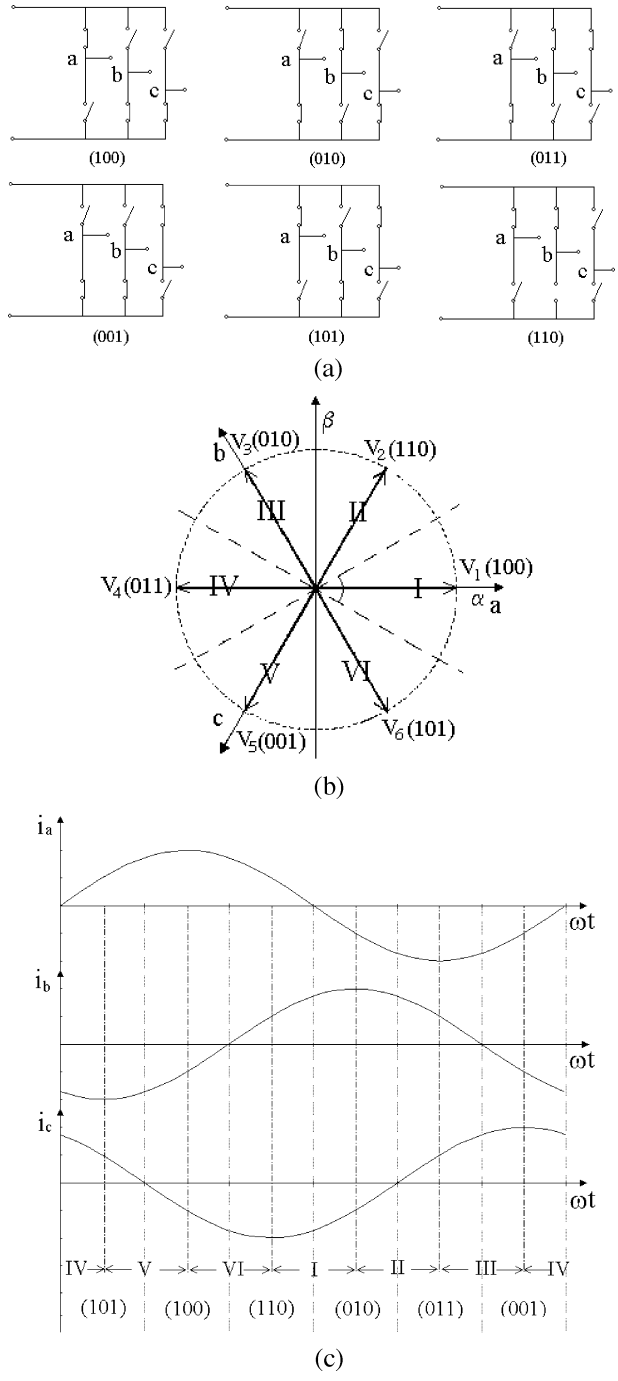

Fig. 2. Nonzero-voltage space vectors for BLAC drive.

Equation (16) is a particular case of (12) when the back-EMF waveform is sinusoidal, or represents the fundamental component of electromagnetic torque when the back-EMF waveform is nonsinusoidal. In general, (12) should be used to calculate the torque when the back-EMF waveform is nonsinusoidal.

As with the application of DTC to BLAC drives [12], its implementation to BLDC drives is based on flux-linkage observers. The stator flux-linkage vector can be obtained from the measured stator voltages $u_{s\alpha}$ and $u_{s\beta}$ and currents $i_{s\alpha}$ and $i_{s\beta}$ as

$$\psi_{s\alpha} = \int (u_{s\alpha} - Ri_{s\alpha})dt \tag{17}$$

$$\psi_{s\beta} = \int (u_{s\beta} - Ri_{s\beta})dt \tag{18}$$

where R is the stator winding resistance. The magnitude and angular position of the stator flux-linkage vector is obtained as

$$\psi = \sqrt{\psi_{s\alpha}^2 + \psi_{s\beta}^2} \tag{19}$$

$$\theta = \arctan \frac{\psi_{s\beta}}{\psi_{s\alpha}}. \tag{20}$$

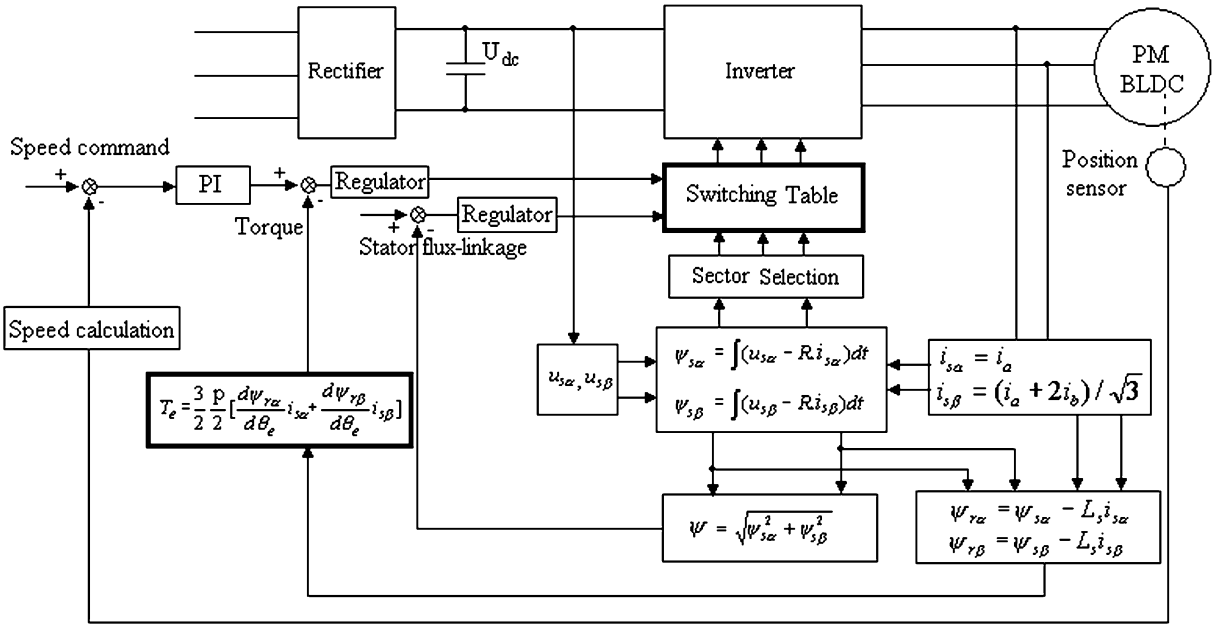

Fig. 3. Schematic of DTC BLDC drive.

The rotor flux linkages can be deduced from the stator flux linkages. For example, for a surface-mounted permanent-magnet rotor, they are given by

$$\psi_{r\alpha} = \psi_{s\alpha} - L_s i_{s\alpha} \tag{21}$$

$$\psi_{r\beta} = \psi_{s\beta} - L_s i_{s\beta} \tag{22}$$

while the torque can be calculated from (12). To simplify the calculation, however, the differential terms in (12) can be pre-determined from the back-EMF waveform assuming that the EMF is proportional to the rotor speed.

Six nonzero-voltage space vectors are defined for a BLDC drive as shown in Fig. 1(a), the sectors of the circular voltage vector which enable the voltage vector to be selected in terms of the stator flux-linkage vector being shown in Fig. 1(b). For comparison, the six nonzero-voltage space vectors and the sectors of the circular voltage vector for a BLAC drive are shown in Fig. 2(a) and (b), respectively. Figs. 1(c) and 2(c) show the idealized phase current waveforms for BLDC and BLAC operation, and their relationship with the voltage space-vector sectors and switching states.

From the foregoing, the main differences between the representation of the voltage space vector in BLAC and BLDC drives are as follows.

1) In a BLAC drive, all three phases are conducting at any instant and the voltage space vectors can be represented by three digits [Fig. 2(a)] which fully represent all the states of the inverter switches, since only one digit is required for each switching leg, as the upper and lower switches operate in tandem mode. In a BLDC drive, however, only two phases are conducting in the 120° conduction mode, except during commutation periods when all three phases conduct, the unexcited phase conducting via a freewheeling diode. Since the upper and lower switches in the same phase leg may both be simultaneously off in BLDC drive, irrespective of the state of the associated freewheel diodes [Fig. 1(a)] six digits are required to represent the states of the inverter switches, one digit for each switch. Thus, the voltage space vectors $V_1, V_2, \ldots V_6$ are represented as switching signals (100 001), (001 001), (011 000), (010 010), (000 110), (100 100), respectively, where, from left to right, the logical values express the

TABLE I
SWITCHING TABLE FOR DTC OF BLDC DRIVE

Torque τ	Flux ϕ	Sector I	II	III	IV	V	VI
1	1	V_1 (100001)	V_2 (001001)	V_3 (011000)	V_4 (010010)	V_5 (000110)	V_6 (100100)
	0	**V_2 (001001)**	**V_3 (011000)**	**V_4 (010010)**	**V_5 (000110)**	**V_6 (100100)**	**V_1 (100001)**
	-1	V_3 (011000)	V_4 (010010)	V_5 (000110)	V_6 (100100)	V_1 (100001)	V_2 (001001)
0	1	V_1 (100001)	V_2 (001001)	V_3 (011000)	V_4 (010010)	V_5 (000110)	V_6 (100100)
	0	**V_0 (000000)**	**V_0 (000000)**	**V_0 (000000)**	**V_0 (000000)**	**V_0 (000000)**	**V_0 (000000)**
	-1	V_3 (011000)	V_4 (010010)	V_5 (000110)	V_6 (100100)	V_1 (100001)	V_2 (001001)

TABLE II
SPECIFICATION OF SURFACE-MOUNTED PERMANENT-MAGNET BRUSHLESS MOTOR

Motor	1	2
Back-emf waveform	Sinusoidal	Non-sinusoidal
Number of poles, p	2	10
Number of slots	3	12
DC link voltage (V)	70	36
Rated speed (rpm)	3000	400
PM excitation flux-linkage (Wb):	0.0928	0.0794
Phase resistance (Ω)	0.466	0.35
Self-inductance (mH)	3.19	4.64
Mutual-inductance (mH)	-1.31	0.0023

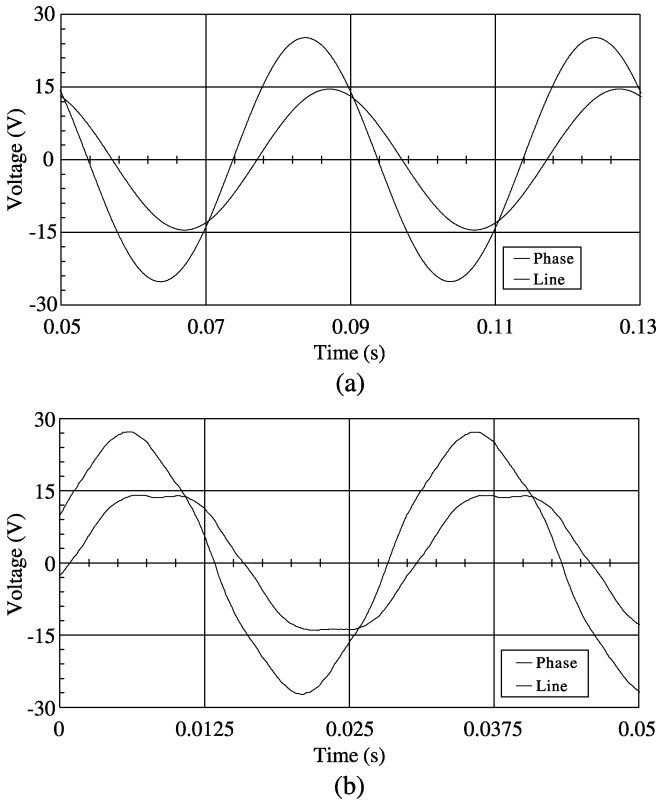

Fig. 4. Back-EMF waveforms. (a) Motor 1. (b) Motor 2.

states of the upper and lower switching signals for phases A, B, and C, respectively. The zero-voltage space vector is defined as (000 000).

2) The voltage space vectors in the α-β reference frame for a BLDC drive have a 30° phase difference relative to those for a BLAC drive, as will be seen by comparing Figs. 1(b) and 2(b). Two nonzero-voltage space vectors now bound each sector of the vector circle, as will be seen in Fig. 1(b), while in a BLAC drive each sector is centered on a nonzero-voltage space vector.

Fig. 3 shows a schematic of a DTC BLDC drive, which is essentially the same as that for a DTC BLAC drive, except for the switching table and torque estimation. By sampling the stator phase currents and voltages and employing a stationary reference transformation, the stator flux linkage in the stationary reference frame can be obtained. The rotor flux linkage in the stationary reference frame can be calculated from (21) and (22), while the magnitude of the stator flux linkage and the electromagnetic torque can be obtained from (19) and (12), respectively. The speed feedback derived from rotor position sensors is compared to the speed command to form the torque command from the proportional–integral (PI) speed regulator. The stator flux-linkage and torque commands are obtained from hysteresis controllers by comparing the estimated electromagnetic torque and stator flux linkage with their demanded values. As can be seen from Table I, the switching pattern of the inverter can be determined according to the stator flux-linkage and torque status from the outputs of two regulators shown in Fig. 3, and the sector in which the stator flux linkage is located at that instant of time. In each sector, if the actual stator flux linkage is the same as the commanded stator flux

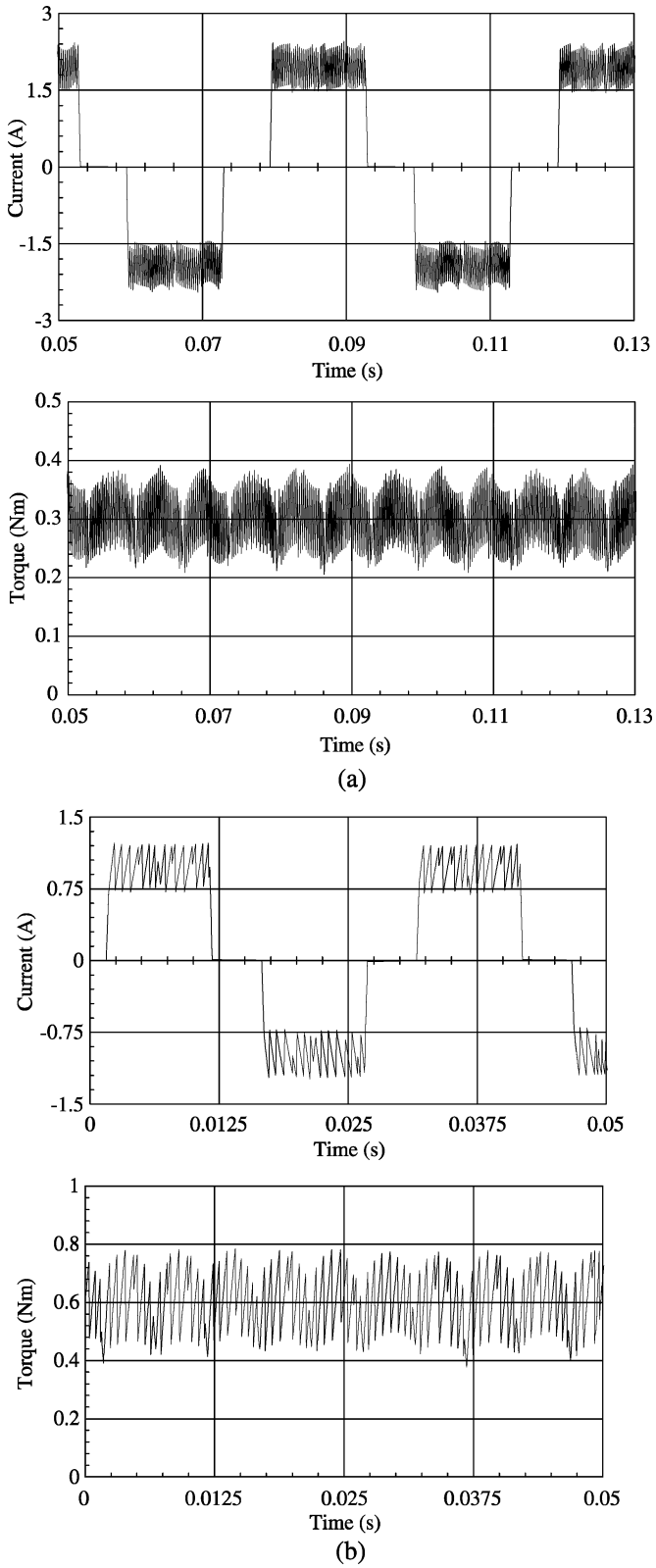

Fig. 5. Current and torque waveforms with conventional PWM current control. (a) Motor 1 (1500 r/min). (b) Motor 2 (400 r/min).

linkage ($\phi = 0$), only one nonzero-voltage space vector and a zero-voltage vector are used to control the increase ($\tau = 1$) or decrease ($\tau = 0$) of the torque, since during any 60° electrical period only two phases are excited and controlled in a BLDC drive,

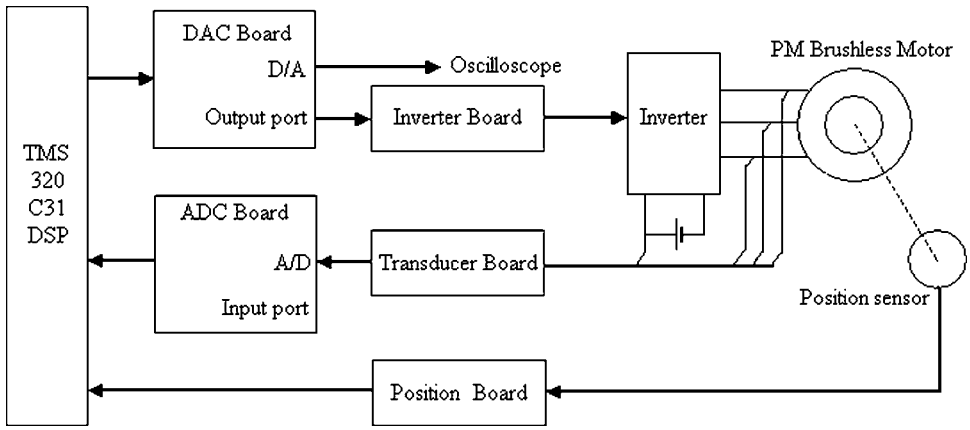

Fig. 6. Schematic of BLDC drive system.

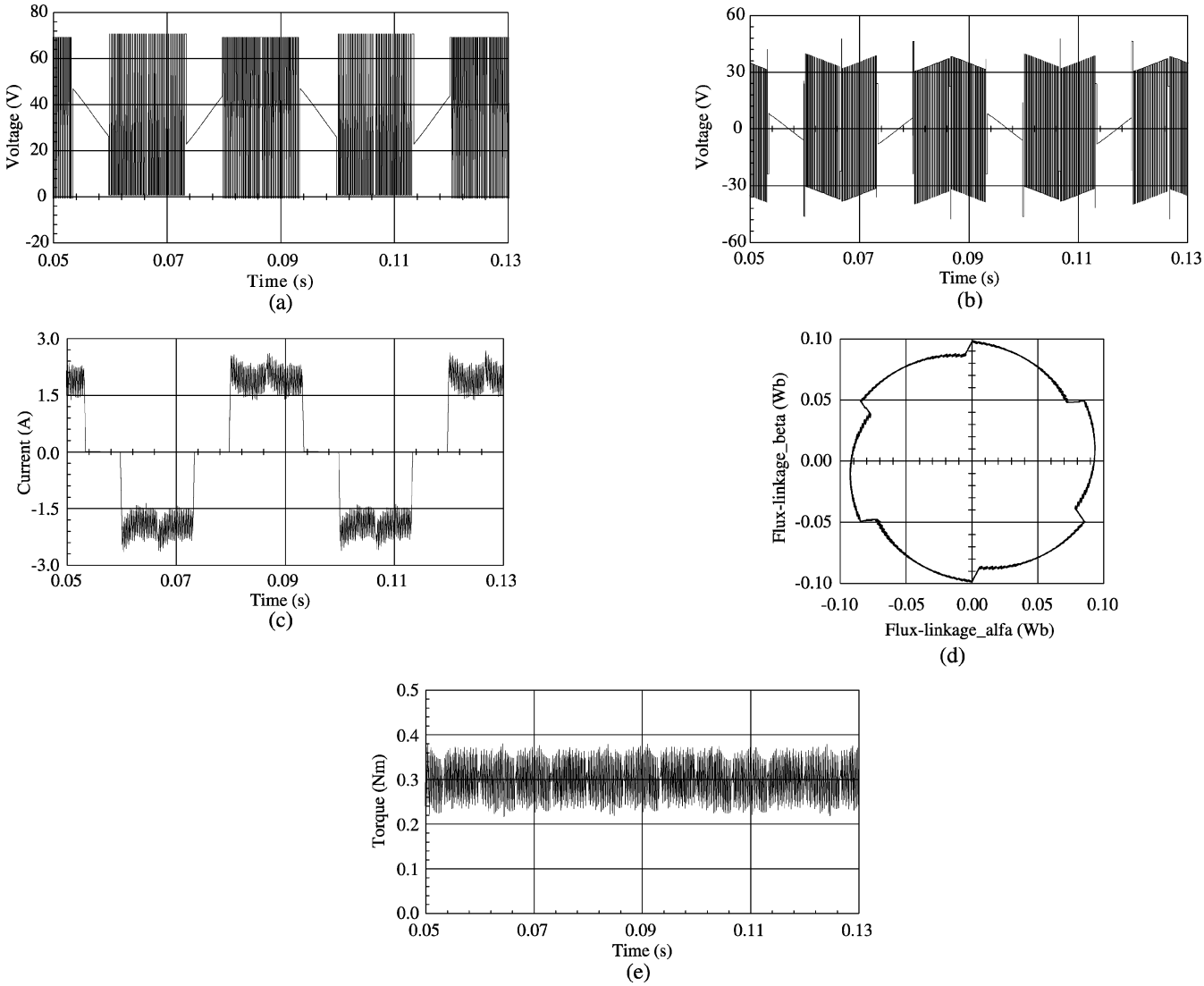

Fig. 7. Simulated results for Motor 1 (1500 r/min). (a) Phase-to-ground voltage. (b) Phase voltage. (c) Phase current. (d) Locus of stator flux linkage. (e) Electromagnetic torque.

as indicated in Table I. In addition, when the actual flux linkage is smaller than the commanded value ($\phi = 1$), the nonzero-voltage space vector is used to increase the flux linkage, while when the actual flux linkage is greater than the commanded value ($\phi = -1$), the nonzero-voltage space vector is used to decrease the stator flux linkage.

In summary, the essential difference between the DTC of BLDC and BLAC drives is in the torque estimation and the

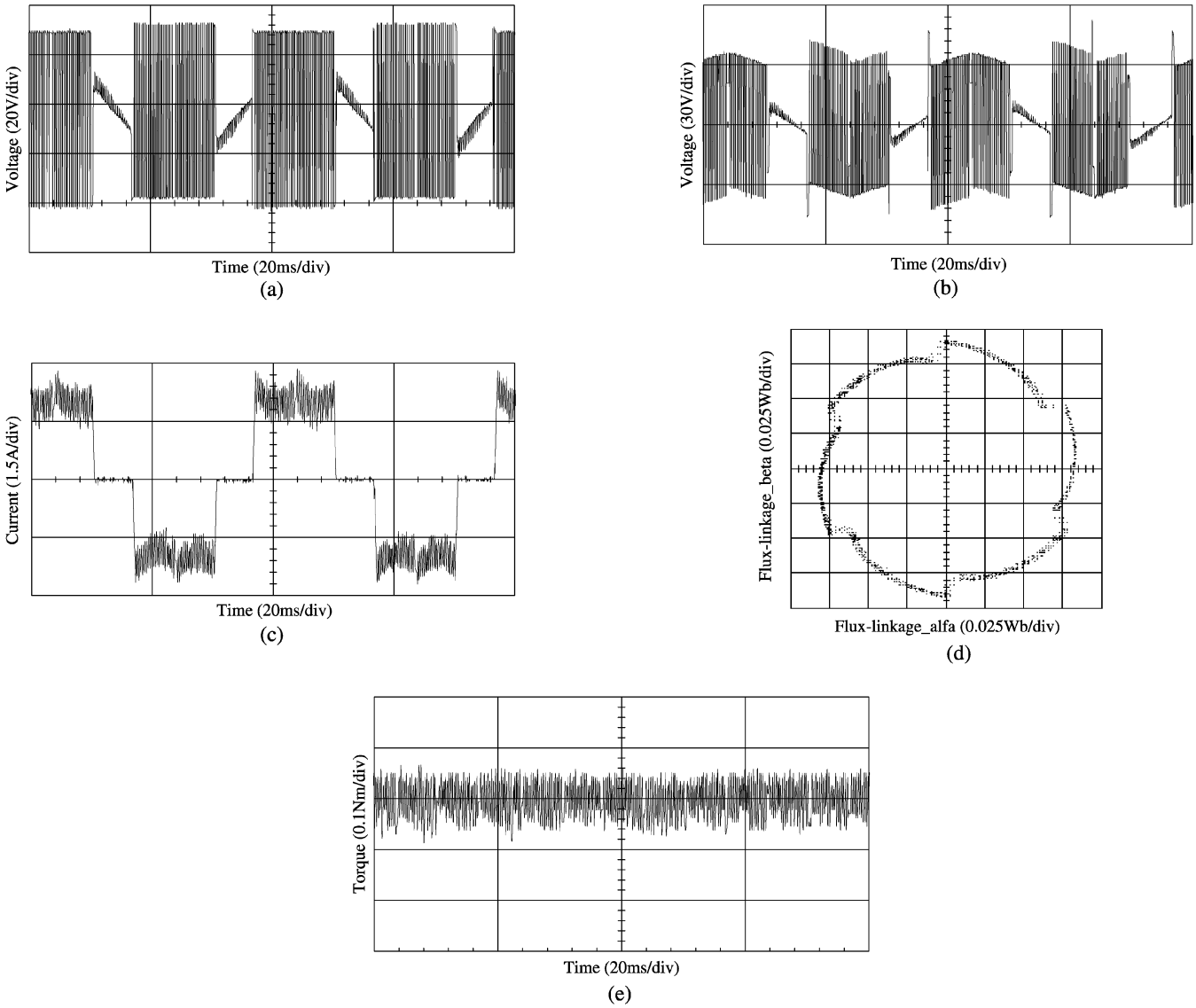

Fig. 8. Experimental results for Motor 1 (1500 r/min). (a) Phase-to-ground voltage. (b) Phase voltage. (c) Phase current. (d) Locus of stator flux linkage. (e) Estimated electromagnetic torque.

representation of the inverter voltage space vectors. However, the control algorithms for the demanded torque, the stator flux linkage, and the output voltage vectors are similar in manner.

III. Simulated and Experimental Results

The utility of the foregoing application of DTC to a BLDC drive has been validated by simulations and measurements on two surface-mounted magnet brushless motors, whose parameters are given in Table II, the motors having significantly different back-EMF waveforms (Fig. 4). Motor 1 has three stator slots, a concentrated winding, and a two-pole diametrically magnetized rotor, a motor topology which is often employed for BLDC drives due to its simplicity [2]. Thus, its air-gap field distribution and back-EMF waveform are inherently sinusoidal. It was selected for investigation since its torque can be estimated from (16), which has the same form as that for a BLAC motor, while conventional PWM current control (constant current demand over 120° electrical) results in a significant low-frequency torque ripple, as shown in the simulated results (Fig. 5) which were obtained by employing a hysteresis controller. Motor 2 also has a concentrated winding and fractional slot and pole number combination, viz. ten poles, 12 slots (its design parameters being given in [17]). However, since its back-EMF waveform is essentially trapezoidal, the torque should be estimated from (12). The main elements of the digital-signal-processor (DSP)-based drive system are shown in Fig. 6. The controller is composed of DAC boards, ADC boards, a rotor position board, a transducer board, and a TMS320C31 DSP, on which the control algorithms are implemented. Each DAC board has four 12-bit digital-to-analog converter (AD767) channels, which are used to output parameters such as the motor speed and phase current, while its output port provides gate drive signals for the switching devices. Each ADC board has four 12-bit analog-to-digital converter (AD678) channels and a 12-bit digital input parallel port. In addition, there are current

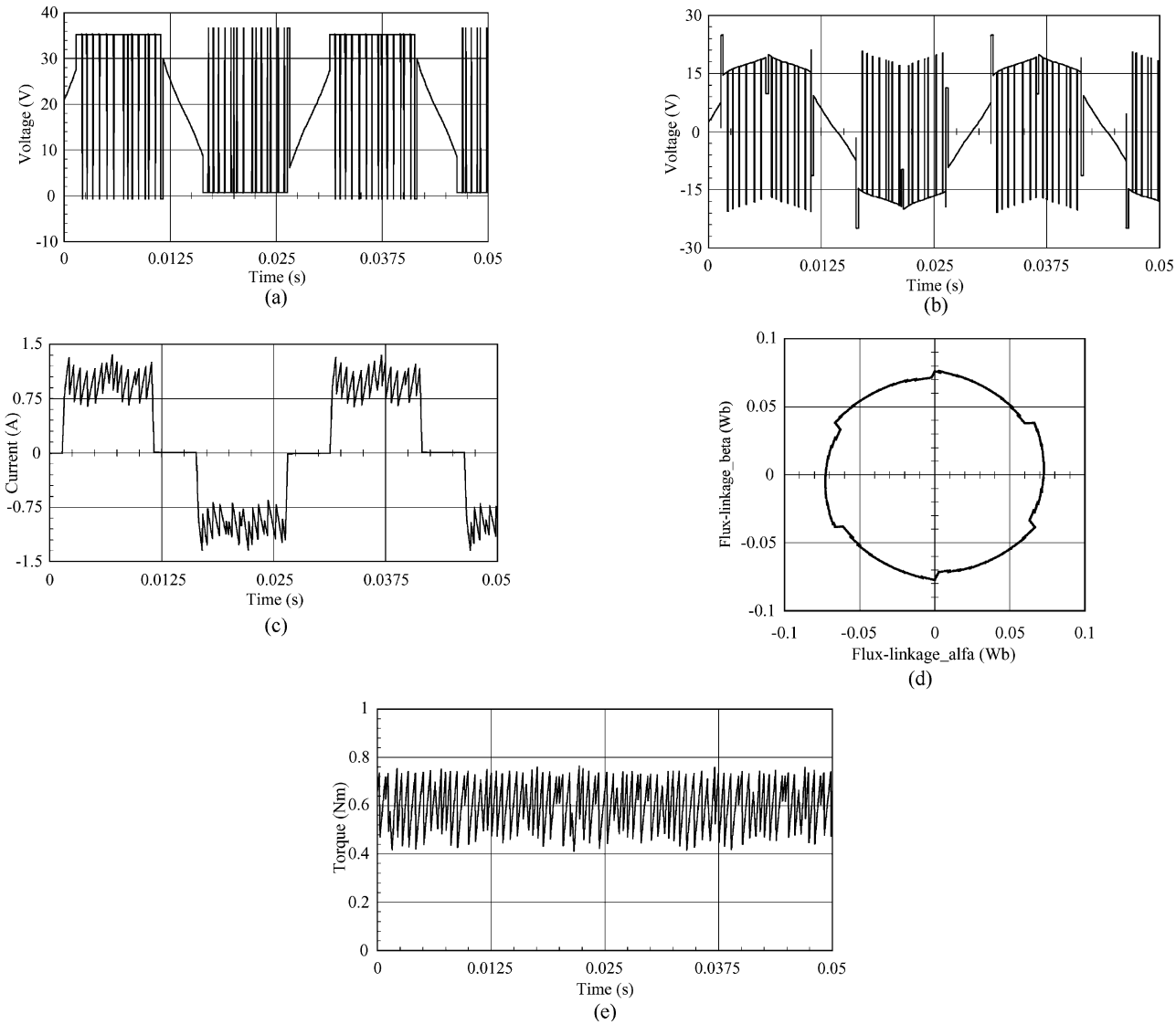

Fig. 9. Simulated results for Motor 2 (400 r/min). (a) Phase-to-ground voltage. (b) Phase voltage. (c) Phase current. (d) Locus of stator flux linkage. (e) Electromagnetic torque.

transducers (LEM LA25-NP) and voltage transducers (LEM LV25-P). The phase currents, and voltages and the inverter dc-link voltage are measured and sampled by the transducer board and ADC board, respectively.

The rotor position board is simply an interface between the DSP and the rotor position sensors, which are simply three Hall devices, the rotor position being obtained by linear interpretation [18]. Although this may introduce a position error, this is not critical for DTC since only the location of the flux-linkage sector is required [10]–[12]. Any dc components in the measured voltages and currents are filtered out using a high-pass filter. Equations (16) and (12) are used in the implementation of DTC for Motors 1 and 2, respectively. A Matlab/Simulink based simulation model has also been used to predict the performance of both motors. By way of example, Figs. 7–10 compare the simulated and measured phase to ground voltage, and the phase voltage and current, the locus of the stator flux linkage, and the estimated electromagnetic torque for both motors.

As will be seen, in general, good agreement is achieved between simulated and measured results. Further, it will be seen that the phase current waveform inherently follows the inverse of the back-EMF waveform within each 60° electrical sector of the 120° electrical conduction period so as to maintain the electromagnetic torque constant. In addition, it should be noted that whilst in a BLAC motor the ideal locus of the stator flux linkage is circular, in a BLDC motor it is noncircular due to the incremental rotation of the stator flux during communication events, which occur every 60° elec. in a 120° electrical conduction BLDC drive. Thus, the flux-linkage locus tends to be hexagonal in shape, as for a six-step drive, the sides being curved due to the influence of the back EMF of the unexcited phase while discrete changes in amplitude occur every 60° electrical due to the action of the freewheeling diodes. Further, it will be noted that, while a high-frequency torque ripple exists in both the simulated and experimental results as a consequence of the low winding inductances and PWM events, the low-frequency torque ripple which would have resulted with conventional vector control havs been eliminated by optimizing the phase current waveform in accordance with the back-EMF waveform.

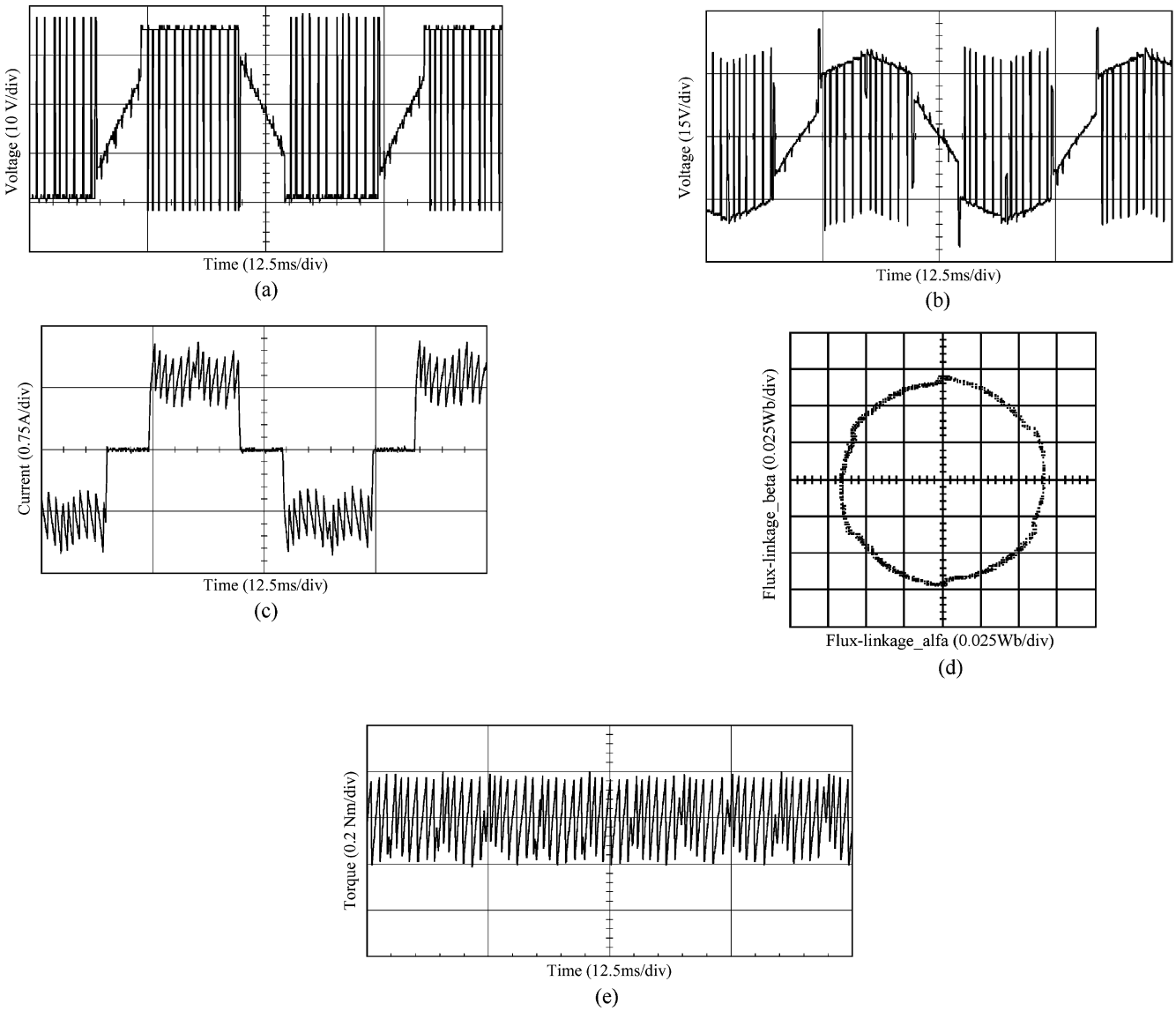

Fig. 10. Experimental results for Motor 2 (400 r/min). (a) Phase-to-ground voltage. (b) Phase voltage. (c) Phase current. (d) Locus of stator flux linkage. (e) Estimated electromagnetic torque.

IV. Conclusion

DTC has been applied to a BLDC drive, and its utility has been validated by simulations and measurements on two BLDC motors which have very different back-EMF waveforms. The main difference between the implementation of DTC to BLAC and BLDC drives is in the estimation of torque and the representation of the inverter voltage vectors. It has been shown that DTC is capable of instantaneous torque control and, thereby, of reducing torque pulsations.

References

[1] J. R. Hendershort Jr and T. J. E. Miller, *Design of Brushless Permanent-Magnet Motors*. Oxford, U.K.: Magana Physics/Clarendon, 1994.

[2] T. Kenjo and S. Nagamori, *Permanent-Magnet and Brushless DC Motors*. Oxford, U.K.: Clarendon, 1985.

[3] P. J. Sung, W. P. Han, L. H. Man, and F. Harashima, "A new approach for minimum-torque-ripple maximum-efficiency control of BLDC motor," *IEEE Trans. Ind. Electron.*, vol. 47, no. 1, pp. 109–114, Feb. 2000.

[4] C. French and P. Acarnley, "Direct torque control of permanent magnet drives," *IEEE Trans. Ind. Appl.*, vol. 32, no. 5, pp. 1080–1088, Sep./Oct. 1996.

[5] T. S. Low, K. J. Tseng, K. S. Lock, and K. W. Lim, "Instantaneous torque control," in *Proc. Fourth Int. Conf. Electrical Machines and Drives*, Sep. 13–15, 1989, pp. 100–105.

[6] T. S. Low, K. J. Tseng, T. H. Lee, K. W. Lim, and K. S. Lock, "Strategy for the instantaneous torque control of permanent-magnet brushless DC drives," in *Proc. IEE—Elect. Power Appl.*, vol. 137, Nov. 1990, pp. 355–363.

[7] T. S. Low, T. H. Lee, K. J. Tseng, and K. S. Lock, "Servo performance of a BLDC drive with instantaneous torque control," *IEEE Trans. Ind. Appl.*, vol. 28, no. 2, pp. 455–462, Mar./Apr. 1992.

[8] S. J. Kang and S. K. Sul, "Direct torque control of brushless DC motor with nonideal trapezoidal back-emf," *IEEE Trans. Power Electron.*, vol. 10, no. 6, pp. 796–802, Nov. 1995.

[9] S. K. Chung, H. S. Kim, C. G. Kim, and M. J. Youn, "A new instantaneous torque control of PM synchronous motor for high-performance direct-drive applications," *IEEE Trans. Power Electron.*, vol. 13, no. 3, pp. 388–400, May 1998.

[10] M. Depenbrock, "Direct self-control of inverter-fed induction machine," *IEEE Trans. Power Electron.*, vol. 3, no. 4, pp. 420–429, Oct. 1988.

[11] I. Takahashi and T. Noguchi, "A new quick-response and high-efficiency control strategies of an induction motor," *IEEE Trans. Ind. Appl.*, vol. 22, no. 5, pp. 820–827, Sep./Oct. 1986.

[12] L. Zhong, M. F. Rahman, W. Y. Hu, and K. W. Lim, "Analysis of direct torque control in permanent magnet synchronous motor drives," *IEEE Trans. Power Electron.*, vol. 12, no. 3, pp. 528–536, May 1997.
[13] I. Boldea and S. A. Nasar, "Torque vector control—a class of fast and robust torque-speed and position digital controllers for electric drives," *Elect. Mach. Power Syst.*, vol. 15, pp. 135–147, 1988.
[14] P. C. Krause, *Analysis of Electric Machinery*. New York: McGraw-Hill, 1987.
[15] V. Gourishankar, *Electromechanical Energy Conversion*. Scranton, PA: International Textbook, 1965.
[16] B. H. Ng, M. F. Rahman, and T. S. Low, "An investigation into the effects of machine parameters on torque pulsation in a brushless dc drive," in *Proc. IEEE IECON'88*, 1988, pp. 749–754.
[17] D. Ishak, Z. Q. Zhu, and D. Howe, "Permanent magnet brushless machines with unequal tooth widths and similar slot and pole numbers," *IEEE Trans. Ind. Appl.*, vol. 41, no. 2, pp. 584–590, Mar./Apr. 2005.
[18] F. G. Capponi, G. De Donato, L. Del Ferraro, O. Honorati, M. C. Harke, and R. D. Lorenz, "AC brushless drive with low resolution hall-effect sensors for an axial flux PM machine," in *Conf. Rec. 39th IEEE-IAS Annu. Meeting*, Oct. 3–7, 2004, pp. 2382–2389.

Yong Liu (S'01) received the B.Eng. and M.Sc. degrees in electrical engineering from Zhejiang University, Hangzhou, China, in 1999 and 2002, respectively. He is currently working toward the Ph.D. degree in the Department of Electronic and Electrical Engineering, University of Sheffield, Sheffield, U.K.

His research interests include control of electrical drives, in particular, the direct torque control of permanent-magnet brushless motors.

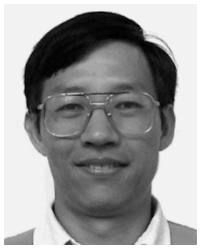

Z. Q. Zhu (M'90–SM'00) received the B.Eng. and M.Sc. degrees from Zhejiang University, Hangzhou, China, in 1982 and 1984, respectively, and the Ph.D. degree from the University of Sheffield, Sheffield, U.K., in 1991, all in electrical and electronic engineering.

From 1984 to 1988, he lectured in the Department of Electrical Engineering, Zhejiang University. Since 1988, he has been with the University of Sheffield, where he is currently a Professor of Electronic and Electrical Engineering. His current major research interests include applications, control, and design of permanent-magnet machines and drives.

Prof. Zhu is a Chartered Engineer in the U.K. and a Member of the Institution of Electrical Engineers, U.K.

David Howe received the B.Tech. and M.Sc. degrees from the University of Bradford, Bradford, U.K., in 1966 and 1967, respectively, and the Ph.D. degree from the University of Southampton, Southampton, U.K., in 1974, all in electrical power engineering.

He has held academic posts at Brunel and Southampton Universities, and spent a period in industry with NEI Parsons Ltd., working on electromagnetic problems related to turbogenerators. He is currently a Professor of Electrical Engineering at the University of Sheffield, Sheffield, U.K., where he heads the Electrical Machines and Drives Research Group. His research activities span all facets of controlled electrical drive systems, with particular emphasis on permanent-magnet excited machines.

Prof. Howe is a Chartered Engineer in the U.K., and a Fellow of the Institution of Electrical Engineers, U.K., and the Royal Academy of Engineering.